Ore Geology Reviews 46 (2012) 60–67

Contents lists available at SciVerse ScienceDirect

Ore Geology Reviews

journal homepage: www.elsevier.com/locate/oregeorev

Pb–Sr–Nd isotope constraints on the fluid source of the Dahu Au–Mo deposit in Qinling Orogen, central China, and implication for Triassic tectonic setting

Zhi-Yong Ni [a], Yan-Jing Chen [a,b,*], Nuo Li [a], Hui Zhang [c]

[a] Key Laboratory of Orogen and Crustal Evolution, Peking University, Beijing, 100871, China
[b] Guangzhou Institute of Geochemistry, Chinese Academy of Sciences, Guangzhou 510640, China
[c] Institute of Geochemistry, Chinese Academy of Sciences, Guiyang 550002, China

ARTICLE INFO

Article history:
Received 3 November 2011
Received in revised form 27 January 2012
Accepted 30 January 2012
Available online 7 February 2012

Keywords:
Sr–Nd–Pb isotope systematics
Ore-forming fluid
The Dahu Au–Mo deposit
Qinling Orogen
Oceanic plate subduction

ABSTRACT

The Dahu Au–Mo deposit is a structure-controlled lode system occurring in the northern Xiaoqinling terrane, Huaxiong Block, Qinling Orogen. This paper reports a new Sr–Nd–Pb isotope dataset obtained for ore sulfides and the hostrocks within the Taihua Supergroup, in an attempt to constrain the source of the ore-forming fluids from a new dimension. 16 sulfide samples yield I_{Sr} ratios of 0.70470–0.71312, with an average of 0.70854; $\varepsilon_{Nd}(t)$ values between −13.5 and −18.1, with average of −15.1; and $(^{206}Pb/^{204}Pb)_i$, $(^{207}Pb/^{204}Pb)_i$ and $(^{208}Pb/^{204}Pb)_i$ ratios of 17.033–17.285, 15.358–15.438, and 37.307–37.582, with averages of 17.162, 15.405, and 37.440, respectively. 5 gneiss samples from the Taihua Supergroup yield I_{Sr} ratios of 0.70947–0.73201, averaging 0.72294; $\varepsilon_{Nd}(t)$ values of −20.0 to −31.1, averaging −25.1; and $(^{206}Pb/^{204}Pb)_i$, $(^{207}Pb/^{204}Pb)_i$, $(^{208}Pb/^{204}Pb)_i$ ratios of 17.127–18.392, 15.416–15.604 and 37.498–37.814, with averages of 17.547, 15.470 and 37.616, respectively. These data show that the ore sulfides have less radiogenic Sr–Nd–Pb isotope systematics than the hostrocks, and suggest that the ore-forming fluids, which interacted with the wallrocks to form ores, must be sourced from a depleted mantle or a depleted, subducted oceanic slab. In combination with the spatial scenario and geochemical signatures of the Triassic magmatites and mineral systems, we argue that in the Triassic the Mianlue Ocean was not completely closed, and that the northward oceanic plate subduction still survived along the Mian-Lue suture, which caused the Late Triassic magmatism and associated mineralization in Qinling Orogen, including the Au–Mo Dahu deposit.

1. Introduction

The East Qinling molybdenum belt (EQMB) is the most important molybdenum province in the world, with the proven reserves of >6 Mt Mo metal (Chen et al., 2000; Li et al., 2011a). It is also a very important metallogenic province for gold, silver, lead and zinc in China (Chen and Fu, 1992; Chen et al., 2009; Jiang et al., 2009; Mao et al., 2002, 2008). The majority of the deposits formed during the Yanshanian Orogeny (Jurassic and Cretaceous), with other deposits being formed before the Jurassic (Chen et al., 2009; Deng et al., 2009; Li et al., 2011a,b).

The Dahu Au–Mo deposit, with reserves of 38 t Au grading 6.8 g/t and 0.1 Mt Mo grading 0.24% (Li et al., 2011a), is ranked as a large-sized Au and Mo deposit, located in the Xiaoqinling terrane (Fig. 1), which is the second largest gold province in China (Chen et al., 1998; Jiang et al., 2009; Kerrich et al., 2000; Mao et al., 2002, 2008; Zhao et al., 2011, 2012). Previous studies have proven it to be an orogenic-type lode system formed by the CO_2-rich, low-salinity fluids (Ni et al., 2008), initially during the Indosinian (Triassic) Orogeny (Li et al., 2008) and later reworked in the Yanshanian (Cretaceous) Orogeny (Li et al., 2011a). As far as we are aware the Dahu deposit is the only recognized orogenic lode in the world with an Au–Mo metal association. However, the source of the ore-forming fluids and metals, as well as genetic mechanism still remains unclear.

The hydrogen–oxygen–sulfur isotope systematics is commonly used to trace the source or origin of the fluids of hydrothermal deposits (Chen et al., 2005, 2008; Hoefs, 1997; Pirajno, 2009; Taylor, 1974; Zheng, 1999). However, in a number of cases H–O–S systematics has been proven nondiagnostic to distinguish fluids originated from magmatic exsolution, metamorphic devolatilization and/or mantle degassing (Hagemann and Cassidy, 2000; Kerrich et al., 2000). Therefore, we try to use other fingerprints, such as Pb–Sr–Nd isotope systematics, to trace the fluid source. In this contribution, we report new Sr, Nd and Pb isotope data obtained from a comprehensive study of the Dahu Au–Mo deposit, and thereby, discuss the sources of ore-forming fluids, and try to put it into a viable tectonic framework.

2. Geology and mineralization

The Qinling Orogen is the central portion of the E–W-trending Central China Orogen (CCO) that evolved from the northernmost

* Corresponding author at: Key Laboratory of Orogen and Crustal Evolution, Peking University, Beijing, 100871, China. Tel.: +86 10 6275 7390.
E-mail address: yjchen@pku.edu.cn (Y.-J. Chen).

0169-1368/$ – see front matter © 2012 Elsevier B.V. All rights reserved.
doi:10.1016/j.oregeorev.2012.01.004

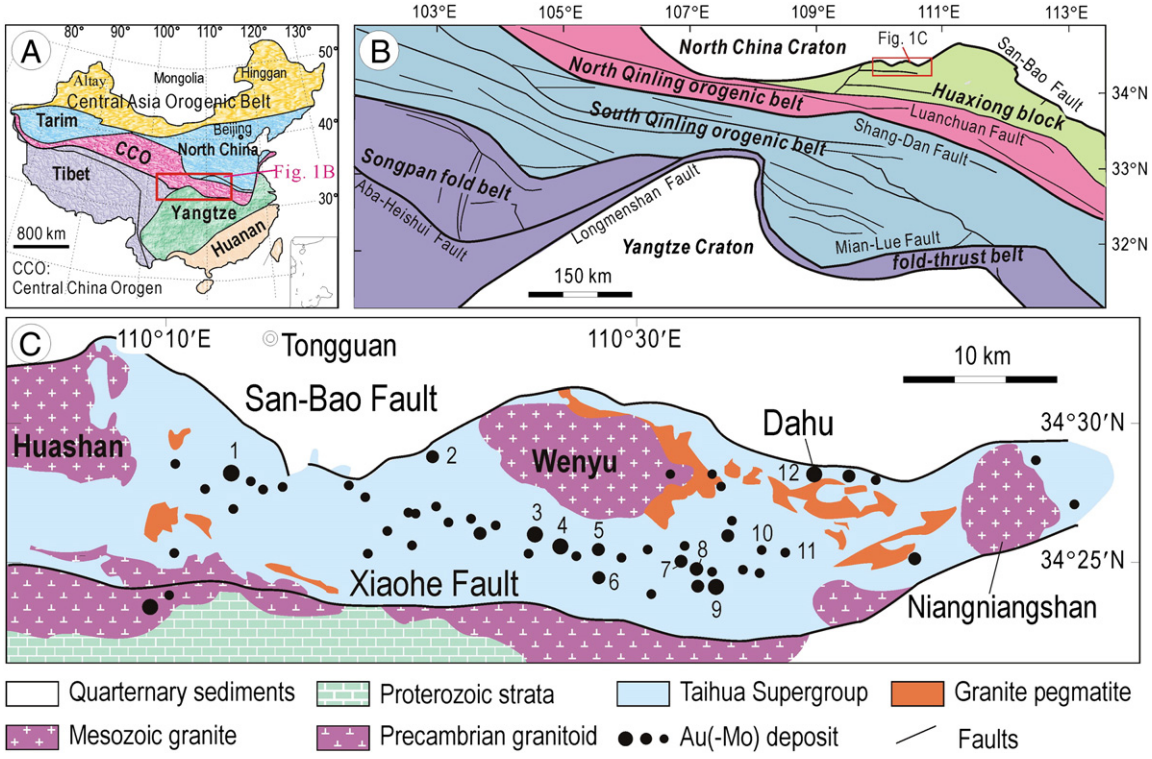

Fig. 1. Geology and distribution of orogenic Au (−Mo) deposits of the Xiaoqinling Terrane. Major gold deposits: 1, Tongguan; 2, Dongtongyu; 3, Wenyu; 4, Dongchuang; 5, Laoyacha; 6, Qiangmayu; 7, Jindongcha; 8, Sifangou; 9, Yangzhaiyu; 10, Donggou; 11, Jinqu; and 12, Dahu.

Paleo-Tethys Ocean and was finally formed by the Mesozoic collision between the North China Craton and continental blocks and terranes that had broken off the Gondwana supercontinent, such as the Yangtze Craton (Fig. 1A, B). The Qinling Orogen has four different tectonic units, which from north to south comprise: the Huaxiong block representing the activitized southern margin of the North China craton, the northern Qinling orogenic belt, southern Qinling orogenic belt, and a foreland fold-thrust belt (e.g. Songpan fold belt) along the northern margin of the Yangtze craton, with the San-Bao, Luanchuan, Shang-Dan, Mian-Lue and Longmenshan faults as their boundaries (Fig. 1B).

The E–W-trending Xiaoqinling terrane, bound by the San-Bao fault to the north and the Xiaohe fault to the south, is one of the Early Precambrian terranes of the Huaxiong Block (Fig. 1C; Li et al., 2011b). The Xiaoqinling terrane is marked by the development of the Taihua Supergroup that hosts the Dahu Au–Mo deposit. The Taihua Supergroup is a suite of amphibolite to granulite facies metamorphic rocks consisting of graphite schists, marbles, quartzites, banded iron-formations, gneisses and amphibolites (Chen and Zhao, 1997). It has been further divided into three groups, namely the 3.0–2.55 Ga Beizi, 2.5–2.3 Ga Dangzehe and 2.3–2.1 Ga Shuidigou Groups (Chen and Zhao, 1997). The Taihua Supergroup was metamorphosed, migmatitized, and intruded by pegmatite dikes in the assembly of the Columbia supercontinent in period of 2.1–1.85 Ga (Li et al., 2011b; Zhao et al., 2009). It was then intruded by the Xiaohe biotite granite of Late Mesoproterozoic, and the Huashan, Wenyu and Niangniangshan biotite granites of Jurassic–Cretaceous (Fig. 1C; Li et al., 2011a; Zhao et al., 2012; and references therein). This suggests that the Xiaoqinling terrane was obviously affected by Mesozoic tectono-magmatic event caused by the Triassic oceanic plate subduction, followed by the Jurassic–Cretaceous continental collision between the Yangtze and North China plates (Chen, 2010; Hu, 1988; Jiang et al., 2010; Xu et al., 2010).

The Dahu Au–Mo deposit is located in the northern margin of the Xiaoqinling terrane, and hosted by migmatite and biotite-plagioclase gneisses of the Taihua Supergroup (Fig. 2A). Gold and molybdenum mineralization are associated with a series of quartz veins controlled by NEE- and NWW-trending and north-dipping faults, namely F1, F8, F7, F35, F5 and F6 from north to south (Fig. 2A). F5 is the widest structural zone, and hosts most of the Dahu orebodies (Fig. 2B). Structural analysis revealed that these faults evolved from Triassic south-directed thrusting to Cretaceous north-directed normal faulting (Zhang et al., 1998, 2009b). Consequently, the quartz veins in these fault zones were deformed, brecciated and/or mylonitized. In the F7 zone, quartz phenocrysts developed with coronal chalcedony quartz or quartz sub-grains domains, and fine-grained molybdenite mostly in matrix cementing quartz or K-feldspar–quartz breccias, containing coarse-grained molybdenite flakes.

According to Li et al. (2011a), the molybdenite at the Dahua deposit occurs as disseminated aggregates in quartz veins and altered wallrocks, spotty flakes within breccias from deformed quartz vein, and thin films on or fine veinlets into breccias or blocks of broken quartz vein. Spatial and textural relationships suggest that coarse-grained molybdenite in deformed orebodies or breccias formed in an earlier mineralization event, whereas fine-grained molybdenite films or veinlets formed in a subsequent remobilization event, resulting in the precipitation of the fine-grained molybdenite. Gold occurs mainly as native gold inclusions in pyrite (Zhao et al., 2011), with minor amounts as inclusions in quartz, or as native gold + pyrite + galena + quartz veinlets filling fissures in cubic pyrite. Minerals coeval with native gold, such as pyrite and galena, show no evidence of structural deformation. According to the mineralogical features, paragenetic associations and crosscutting relationships of veinlets, the hydrothermal process forming the Dahu mineral system is divided into four stages marked by, from early to late, (1) deformed or brecciated, coarse-grained K-feldspar − quartz ± molybdenite ± pyrite veins; (2) fine-grained quartz − molybdenite − pyrite − gold films or variably grained aggregate disseminations; (3) quartz − polymetallic sulfide − gold veins containing chalcopyrite, pyrite, galena, sphalerite and other metallic minerals; and (4) quartz-carbonate veins occasionally containing

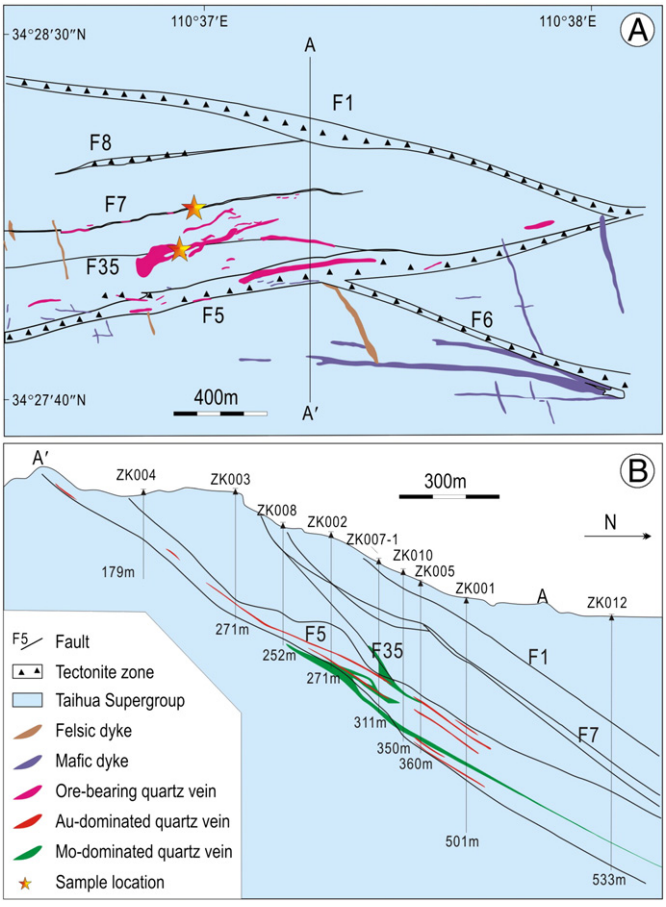

Fig. 2. Geological map of the Dahu Au–Mo deposit (from Li et al., 2011a). (A) Simplified geological map at the 500-meter level, showing the occurrences of ore-bearing quartz veins and their relation to faults such as F5, F7 and S35; (B) Cross-section A–A′ in (A), showing the distribution of Au- and Mo-dominated orebodies hosted by F5.

pyrite. Thus, two Mo-mineralization stages are revealed, with the former represented by coarse-grained molybdenite, and the latter by fine-grained molybdenite films; and native gold grains can be observed in pyrite or quartz of stages 2 and 3. Sometimes, stages 2 and 3 are totally called "main mineralization stage" (e.g., Zhao et al., 2012).

The SHRIMP U–Th–Pb dating of hydrothermal monazite intergrown with early-stage molybdenite yielded an initial precipitation age of 216 ± 5 Ma (Li et al., 2011a), which is identical to the molybdenite Re–Os isochron age of 218 ± 41 Ma (Li et al., 2008) and suggests that the Dahu deposit was firstly formed in Late Triassic, i.e., Indosinian Orogeny. The monazite also yielded SHRIMP U–Th–Pb ages clustering 185–135 Ma, with minimum value of 125 Ma, suggesting that the Dahu mineral system was reworked by a Yanshanian tectono-thermal event that resulted in large-scale gold mineralization in the Xiaoqinling terrane (Li et al., 2011a). However, no mineralogical and petrographical difference has been identified between the monazite grains with different ages, and therefore, it is inferred that the younger monazite was formed at the expense of the older ones during the Yanshanian Orogeny, probably during a single event that occurred at ~125 Ma.

3. Samples and analytical methods

The samples were collected from the S35 quartz vein and the F7 altered tectonite zone, from which seven pyrite, four molybdenite, three galena and two chalcopyrite mineral samples were separated. In addition, five samples of unaltered gneisses of the Taihua Supergroup were collected at the deposit area. Sr, Nd, and Pb isotopic analyses were performed at the Analytical Laboratory of the Beijing Research Institute of Uranium Geology, China. Sample powders were dissolved in $HF + HNO_3 + HClO_4$ mixture. Digested samples were dried and redissolved in 6 N HCl, dried again and redissolved in 0.5 N HCl (for Sr and Nd separation) or 0.5 N HBr (for Pb separation). Sr and Nd fractions were separated following standard chromatographic techniques using AG50x8 and PTFE–HDEHP resins with HCl as eluent, whilst Pb fraction was separated using strong alkali anion exchange resin with HBr and HCl as eluents.

All isotopic measurements were made by thermal ionization mass spectrometry using ISOPROBE-T mass spectrometer. $^{87}Sr/^{86}Sr$ isotope ratios were normalized to $^{86}Sr/^{88}Sr = 0.1194$ and $^{143}Nd/^{144}Nd$ isotope ratios to $^{146}Nd/^{144}Nd = 0.7219$. The JNdi Nd-Standard yielded $^{143}Nd/^{144}Nd$ ratios of 0.512118 ± 03 (reference value 0.512115 ± 7, Tanaka et al., 2000) and the NBS 987 Sr standard yielded $^{87}Sr/^{86}Sr$ ratios of 0.710250 ± 07 (reference value 0.710248). A factor of 1‰ per mass unit for instrumental mass fractionation was applied to

Table 1
The Sr isotope ratios of sulfides and Taihua Supergroup from the Dahu deposit.

Sample no.	Samples	Rb (ppm)	Sr (ppm)	$^{87}Sr/^{86}Sr$	$^{87}Rb/^{86}Sr$	$I_{sr\text{-}125Ma}$	$I_{sr\text{-}218Ma}$
7-002-2	Chalcopyrite	0.37	4.82	0.713662	0.222233	0.71327	0.71297
7-005-3	Chalcopyrite	0.17	1.33	0.713904	0.372228	0.71324	0.71275
DH-3	Pyrite	0.40	12.5	0.706199	0.092111	0.70604	0.70591
DH07-1	Pyrite	0.44	12.8	0.707688	0.099685	0.70751	0.70738
DH07	Pyrite	0.51	10.4	0.707943	0.142445	0.70769	0.70750
DH04	Pyrite	0.56	1.22	0.712082	1.335784	0.70971	0.70794
7-005-1	Pyrite	0.34	0.43	0.713779	2.297252	0.70970	0.70666
7-002-1	Pyrite	0.31	3.15	0.714003	0.285837	0.71350	0.71312
35-010-1	Pyrite	0.30	9.57	0.706434	0.090690	0.70627	0.70615
DH-4	Galena	1.07	1.16	0.712976	2.670247	0.70823	0.70470
DH08-20	Galena	0.52	4.01	0.711336	0.371722	0.71068	0.71018
35-010-2	Galena	0.32	3.06	0.707481	0.304457	0.70694	0.70654
DH08-04	Molybdenite	6.05	156	0.710481	0.112241	0.71028	0.71013
DH08-21	Molybdenite	2.03	28.2	0.707858	0.208284	0.70749	0.70721
DH08-22	Molybdenite	0.49	120	0.707269	0.011862	0.70725	0.70723
DH08-23	Molybdenite	2.11	32.7	0.710827	0.186754	0.71050	0.71025
Average	Sulfides					0.70927	0.70854
DH08-08	Taihua SGp	107	226	0.716458	1.371036	0.71402	0.70947
DH08-12	Taihua SGp	200	272	0.716072	2.129208	0.71229	0.71221
DH08-15	Taihua SGp	140	282	0.736418	1.440452	0.73386	0.72906
DH08-16	Taihua SGp	168	306	0.733996	1.592594	0.73117	0.72906
ZK-628	Taihua SGp	131	379	0.735122	1.002760	0.73334	0.73201
Average	Taihua SGp					0.72494	0.72236

the Pb analyses, using NBS 981 as reference material. Measurement of the common-lead standard NBS 981 gave average values of $^{208}Pb/^{206}Pb = 2.1681 \pm 0.0008$; $^{207}Pb/^{206}Pb = 0.91464 \pm 0.00033$; and $^{204}Pb/^{206}Pb = 0.059042 \pm 0.000037$ with uncertainties of <0.1% at the 95% confidence level.

4. Results

The results of Sr, Nd, and Pb isotopic analyses are listed in Tables 1–3, respectively. The ratios of $^{87}Rb/^{86}Sr$, $^{147}Sm/^{144}Nd$, $^{238}U/^{204}Pb$, $^{235}U/^{204}Pb$, and $^{232}Th/^{204}Pb$ were calculated according to the contents of Rb, Sr, Sm, Nd, U, Th and Pb, and the measured isotope ratios of the samples. Given that the molybdenite Re–Os isochron age of 218 Ma (Li et al., 2008) and the minimum SHRIMP monazite U–Th–Pb age of 125 Ma (Li et al., 2011a) represent the ore-forming and thermal reworking ages, respectively, to accurately study the source of the fluids and metals using the isotope tracers, the Sr, Nd and Pb isotope ratios of the samples at 218 Ma and 125 Ma were calculated, and reported as I_{Sr}, εNd(t), $(^{208}Pb/^{204}Pb)i$, $(^{207}Pb/^{204}Pb)i$, and $(^{206}Pb/^{204}Pb)i$, respectively (Tables 1–3). The chondrite $(CHUR)_{Nd}$ parameters used in the calculation are $^{143}Nd/^{144}Nd = 0.512638$ and $^{147}Sm/^{144}Nd = 0.1967$ (Jacobsen and Wasserburg, 1980), respectively.

5. Discussion

The calculated results for 218 Ma and 125 Ma are very similar, and do not significantly differ from the measured values (Tables 1–3), suggesting that the conclusions drawn for fluid source from these datasets will be similar too. It is not in need to trace fluid source using each dataset. Hereafter we will only discuss the fluid source and tectonic setting using the dataset of 218 Ma, considering the mineral system is holistically of Late Triassic age.

5.1. Source of the ore-forming fluids

It is well known that many hydrothermal ore deposits are formed by interaction of ore-fluids with wallrocks; and therefore the isotopic fingerprint of the ores depends on the isotope compositions of the wallrocks and the ore-forming fluids (Chen et al., 2008; Pirajno, 2009). Thus, if we know the isotope compositions of the unaltered wallrocks and the ores, we can infer the isotope compositions of the ore-forming fluids.

The I_{Sr} values of sulfide samples from the Dahu deposit range from 0.70470 to 0.71312, and average 0.70854 (Table 1; Fig. 3), demonstrating a two end-member mixing isotopic composition of crust and mantle. The I_{Sr} ratios of five ore-hosting gneisses of the Taihua Supergroup are between 0.70947 and 0.73201, with an average of 0.72236 (Table 1), undoubtedly showing a strontium isotopic nature of the upper continental crust. Because the average I_{Sr} value of ore sulfides is lower than the minimum I_{Sr} ratio, and much lower than the average I_{Sr} value of the ore-hosting Taihua Supergroup, a low I_{Sr} fluid system is a prerequisite to form the sulfides with I_{Sr} values of 0.70470–0.71312. The I_{Sr} ratios of the fluids that interacted with the wallrocks are no higher than 0.70470, which is the lowest I_{Sr} ratio of sulfides. This shows that the fluids forming the Dahu deposit must be initially sourced from a depleted mantle or from a source compositionally similar to depleted mantle (Fig. 3).

The $(^{143}Nd/^{144}Nd)_i$ ratios of ore sulfides range from 0.51143 to 0.51215, and average 0.51158, obviously higher than those of the Taihua Supergroup (0.51076–0.51133, averaging 0.51107; Table 2). The $\varepsilon_{Nd}(t)$ values of the sulfides are between −13.5 and −18.1, with average of −15.1, also higher than those of the Taihua Supergroup (−20.0 to −31.1, with average of −25.1). The fluids, which interacted with the Taihua Supergroup gneisses to form the ore sulfides, must have $(^{143}Nd/^{144}Nd)_i$ and $\varepsilon_{Nd}(t)$ values no lower than 0.51215 and −13.5, respectively. Hence the fluids were likely sourced from a mantle, same with the result indicated by the I_{Sr} values (Fig. 3).

The $(^{206}Pb/^{204}Pb)_i$, $(^{207}Pb/^{204}Pb)_i$ and $(^{208}Pb/^{204}Pb)_i$ values for sulfides are 17.033–17.285, 15.358–15.438 and 37.307–37.582, respectively, with averages of 17.162, 15.405 and 37.440, respectively (Table 3). These values are nearly same to the $^{206}Pb/^{204}Pb$, $^{207}Pb/^{204}Pb$ and $^{208}Pb/^{204}Pb$ ratios of the sulfides which have very low contents of U and Th relative to Pb. The $(^{206}Pb/^{204}Pb)_i$, $(^{207}Pb/^{204}Pb)_i$ and $(^{208}Pb/^{204}Pb)_i$ values of the gneisses range 17.127–18.392, 15.416–15.604 and 37.498–37.814, and average 17.547, 15.470 and 37.616, respectively. It is clear that the Pb isotope ratios of the Taihua Supergroup at 218 Ma are higher and more variable than those of the ore sulfides, implying that the Pb-isotope ratios of the ore-forming fluids must be lower than the lowest Pb-isotope ratios of the sulfides (Fig. 4). Hence the ore-forming fluids were likely sourced from the mantle or an equivalent composition.

The abovementioned results indicate that the ore-forming fluids possibly had $\varepsilon_{Nd}(t) > -13.5$, $I_{Sr} < 0.7047$, $(^{206}Pb/^{204}Pb)_i < 17.033$,

Table 2
The Nd isotope ratios of sulfides and Taihua Supergroup from the Dahu deposit.

Sample no.	Sample	Sm (ppm)	Nd (ppm)	$^{143}Nd/^{144}Nd$	$^{147}Sm/^{144}Nd$	$(^{143}Nd/^{144}Nd)_i$	$f_{Sm/Nd}$	$\varepsilon_{Nd}(125)$	$\varepsilon_{Nd}(218)$
7-002-2	Chalcopyrite	0.06	0.62	0.511674	0.0595	0.51159	−0.70	−16.6	−15.0
7-005-3	Chalcopyrite	0.01	0.06	0.511842	0.1228	0.51167	−0.38	−14.4	−13.5
DH-3	Pyrite	0.43	4.42	0.511737	0.0583	0.51165	−0.70	−15.4	−13.7
DH07-1	Pyrite	0.13	1.16	0.511675	0.0657	0.51158	−0.67	−16.7	−15.1
DH07	Pyrite	0.09	0.37	0.511743	0.1520	0.51153	−0.23	−16.8	−16.2
7-005-1	Pyrite	0.01	0.12	0.511625	0.0526	0.51155	−0.73	−17.5	−15.8
7-002-1	Pyrite	0.02	0.12	0.511674	0.1025	0.51153	−0.48	−17.3	−16.2
35-010-1	Pyrite	0.08	0.62	0.511764	0.0765	0.51165	−0.61	−15.1	−13.7
DH-4	Galena	0.03	0.11	0.511848	0.1711	0.51160	−0.13	−15.0	−14.7
DH08-20	Galena	0.37	3.06	0.511662	0.0727	0.51156	−0.63	−17.1	−15.6
35-010-2	Galena	0.17	1.21	0.511551	0.0839	0.51143	−0.57	−19.4	−18.1
DH08-04	Molybdenite	44	379	0.511642	0.0705	0.51154	−0.64	−17.4	−15.9
DH08-21	Molybdenite	51	429	0.511764	0.0731	0.51166	−0.63	−15.1	−13.6
DH08-22	Molybdenite	156	1566	0.511727	0.0602	0.51164	−0.69	−15.6	−14.0
DH08-23	Molybdenite	67	368	0.511703	0.1115	0.51154	−0.43	−16.9	−15.9
Average	Sulfides					0.51158	−0.55	−16.4	−15.1
DH08-08	Taihua SGp	8.70	16.3	0.511400	0.3226	0.51094	0.64	−26.2	−27.7
DH08-12	Taihua SGp	5.89	25.6	0.511361	0.1391	0.51116	−0.29	−24.0	−23.3
DH08-15	Taihua SGp	15.6	111	0.510886	0.0849	0.51076	−0.57	−32.4	−31.1
DH08-16	Taihua SGp	3.06	15.7	0.511501	0.1178	0.51133	−0.40	−20.9	−20.0
ZK-628	Taihua SGp	1.96	10.3	0.511313	0.1150	0.51115	−0.42	−24.6	−23.6
Average	Taihua SGp					0.51107	−0.21	−25.6	−25.1

Table 3
The Pb isotope composition of sulfides and Taihua Supergroup from the Dahu deposit.

No.	Sample	Pb (ppm)	Th (ppm)	U (ppm)	$^{208}Pb/^{204}Pb$ Today	$^{207}Pb/^{204}Pb$ Today	$^{206}Pb/^{204}Pb$ Today	$^{208}Pb/^{204}Pb$ 125 Ma	$^{207}Pb/^{204}Pb$ 125 Ma	$^{206}Pb/^{204}Pb$ 125 Ma	$^{208}Pb/^{204}Pb$ 218 Ma	$^{207}Pb/^{204}Pb$ 218 Ma	$^{206}Pb/^{204}Pb$ 218 Ma
7-002-2	cpy	2602	0.174	0.161	37.484	15.402	17.147	37.484	15.402	17.147	37.484	15.402	17.147
7-005-3	cpy	81,599	0.023	0.017	37.372	15.358	17.033	37.372	15.358	17.033	37.372	15.358	17.033
DH-3	Pyrite	4664	0.162	0.029	37.307	15.397	17.230	37.307	15.397	17.230	37.307	15.397	17.230
DH07-1	Pyrite	2032	0.081	0.025	37.479	15.400	17.161	37.479	15.400	17.161	37.479	15.400	17.161
DH07	Pyrite	9674	0.040	0.020	37.478	15.400	17.158	37.478	15.400	17.158	37.478	15.400	17.158
DH04	Pyrite	4049	0.033	0.015	37.474	15.395	17.077	37.474	15.395	17.077	37.474	15.395	17.077
7-005-1	Pyrite	20,829	0.032	0.021	37.447	15.387	17.084	37.447	15.387	17.084	37.447	15.387	17.084
7-002-1	Pyrite	696	0.032	0.025	37.498	15.415	17.158	37.498	15.415	17.158	37.498	15.415	17.158
35-010-1	Pyrite	6999	0.022	0.033	37.379	15.410	17.223	37.379	15.410	17.223	37.379	15.410	17.223
DH-4	Galena	642,147	0.080	0.017	37.536	15.417	17.110	37.536	15.417	17.110	37.536	15.417	17.110
DH08-20	Galena	768,471	0.223	1.580	37.582	15.438	17.126	37.582	15.438	17.126	37.582	15.438	17.126
35-010-2	Galena	681,027	0.067	0.164	37.380	15.411	17.222	37.380	15.411	17.222	37.380	15.411	17.222
DH08-04	Mo	3718	19.40	1.030	37.376	15.421	17.286	37.374	15.421	17.286	37.372	15.421	17.285
DH08-21	Mo	14,120	16.40	1.680	37.441	15.415	17.195	37.441	15.415	17.195	37.440	15.415	17.195
DH08-22	Mo	55,906	54.10	10.20	37.436	15.395	17.135	37.436	15.395	17.135	37.435	15.395	17.135
DH08-23	Mo	5008	22.00	4.370	37.376	15.414	17.255	37.374	15.414	17.254	37.373	15.414	17.253
Average	Sulfide							37.440	15.405	17.162	37.440	15.405	17.162
DH08-08	Taihua	63	4.400	2.670	37.863	15.454	17.548	37.835	15.451	17.496	37.814	15.449	17.457
DH08-12	Taihua	159	1.780	1.050	37.506	15.429	17.272	37.502	15.429	17.264	37.498	15.428	17.258
DH08-15	Taihua	67	21.60	1.300	49.758	15.606	18.441	49.606[a]	15.605	18.413	49.492[a]	15.604	18.392
DH08-16	Taihua	73	0.490	0.300	37.538	15.454	17.511	37.535	15.454	17.506	37.533	15.454	17.502
ZK-628	Taihua	378	14.60	2.030	37.645	15.417	17.138	37.630	15.417	17.132	37.618	15.416	17.127
Average	Taihua							37.625	15.471	17.562	37.616	15.470	17.547

Abbreviations: cpy, chalcopyrite; Mo, molybdenite; Taihua, Taihua Supergroup.
[a] The $^{208}Pb/^{204}Pb$ of sample DH08-16 is abnormally higher than other samples, and therefore not included in the averages of $(^{208}Pb/^{204}Pb)_{125,}$ and $(^{208}Pb/^{204}Pb)_{218}$.

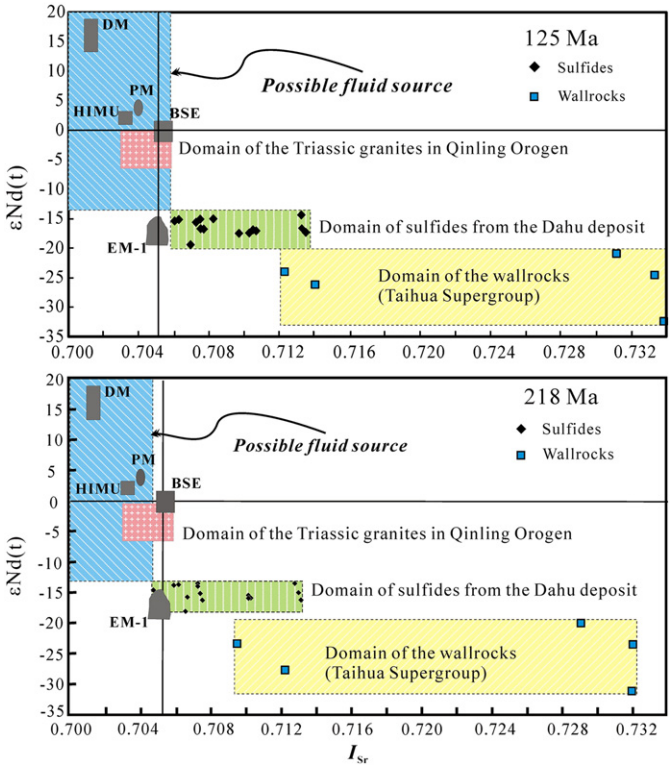

Fig. 3. The εNd(t) vs. I_{Sr} plots of the Dahu Au–Mo deposit (the base map from Depaolo and Wasserburg, 1979). Abbreviations: DM, depleted mantle; PM, primitive mantle; HIMU, high U/Pb mantle; EM-1, enriched mantle I; BSE, bulk silicate earth.

($^{207}Pb/^{204}Pb)_i$ <15.358, and ($^{208}Pb/^{204}Pb)_i$ <37.307, and were likely sourced from the mantle. This inference is clearly illustrated in Fig. 3. In this figure, the inferred I_{Sr} and $\varepsilon_{Nd}(t)$ values of the fluids overlap the domain ($\varepsilon_{Nd}(t) = -0.2$ to -6.3, $I_{Sr} = 0.7030$–0.7059; Jiang et al., 2010) of the Triassic granites in Qinling Orogen.

5.2. Metallogenesis and tectonic setting

According to Li et al. (2011a and references therein), the Dahu Au–Mo deposit is a structurally controlled orogenic-type lode system initially formed during the Indosinian Orogeny and later overprinted by events linked with the Yanshanian Orogeny, at about 140 to 100 Ma. The Yanshanian tectonic setting in Qinling Orogen was universally interpreted as syn- to post-collision tectonism, which resulted in widespread magmatism and hydrothermal mineralization (Chen and Fu, 1992; Chen et al., 2009; Jiang et al., 2009; Mao et al., 2008). As an example, in the Xiaoqinling area all the Mesozoic granites and most of the mineral systems were formed in Yanshanian Orogeny (see above).

For a long time, the Indosinian Orogeny in Qinling Orogen was also interpreted to be syn- to post-collision tectonism by many geologists (Chen and Fu, 1992; Hu, 1988; Mao et al., 2008; Zhang et al., 2001, 2002; Zhu et al., 2011), through correlating Qinling Orogen to Dabie Shan. Recently, a group of geologists (e.g. Chen, 2010; Chen et al., 2009; Jiang et al., 2010; Li et al., 2007, 2011a; Xu et al., 2010; Zhang et al., 2009a) proved that in the Triassic the Mian-Lue Ocean had not completely closed yet and that the oceanic plate was still being subducted northward beneath the southern and northern Qinling orogenic belts, and the Huaxiong Block (Fig. 5). This oceanic plate subduction resulted in, as evidenced by magmatism and metallogenic processes occurring in the Triassic in the Qinling Orogen (Fig. 5), from south to north: (1) the peraluminous, and B- and P-rich S-type granite dykes (ca. 220 Ma) in the Yangshan gold field, which originated from partial melting of the accretionary sediment prisms in fore-arc basin (Chen, 2010; Liu et al., 2008; Zhang et al., 2009a); (2) the widely developed high Mg#, high εNd(t), low I_{Sr}, calc-alkaline I-type granites in the southern and northern Qinling orogenic belts (Jiang et al., 2010), which were typically formed in a magmatic arc during 227–211 Ma; (3) the alkaline granites (Gong et al., 2009) associated with HREE-enriched carbonatite dykes in the northern Qinling orogenic belt and the Huaxiong Block, which, represented by the carbonatite dykes (221 Ma) in the Huanglongpu Mo field (Xu et al., 2010), are interpreted to have originated from low-grade partial melting of the refractory, subducted oceanic slab or depleted mantle; and (4) the Dahu Au–Mo deposit at the northern margin of the Huaxiong Block, which has similar ages and similar isotope compositions to the former three kinds of geologic bodies, and therefore, have been initially formed by the fluids sourced from the metamorphic devolatilization of the refractory, subducted oceanic slab. These fluids, possibly originated from rocks of eclogite facies, must be dominated by CO_2, instead of water, and are difficult to cause partial melting of silicate minerals in mantle or lower crust, but easy to migrate upward to upper crust to cause orogenic-type mineralizations.

6. Conclusions

(1) The Dahu Au–Mo deposit is structure-controlled lode system developed at ca. 218 Ma. The Sr–Nd–Pb isotope systematics of the ore sulfides from the Dahua deposit are far less radiogenic compared to those of the hostrocks within the Early Precambrian Taihua Supergroup. The initial ore-forming fluids forming the Dahu deposit were sourced from a depleted mantle or a refractory, subducted oceanic slab, beneath the Xiaoqinling area.

(2) In Qinling Orogen, the tectonic framework and geochemical signatures of the Triassic magmatites and mineral systems, including the Au–Mo Dahu deposit, can be interpreted by a

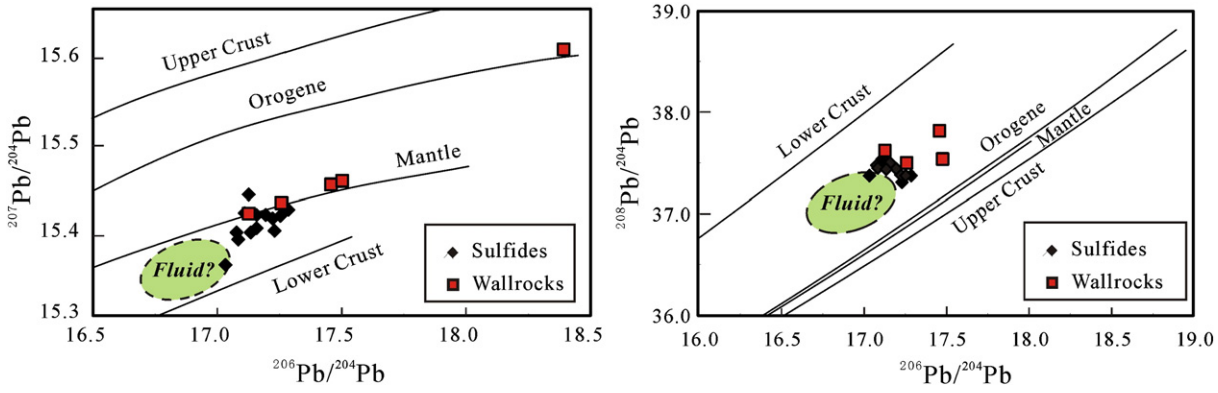

Fig. 4. The plumbotectonic model for the Dahu Au–Mo deposit (the base map from Zartman and Doe, 1981).

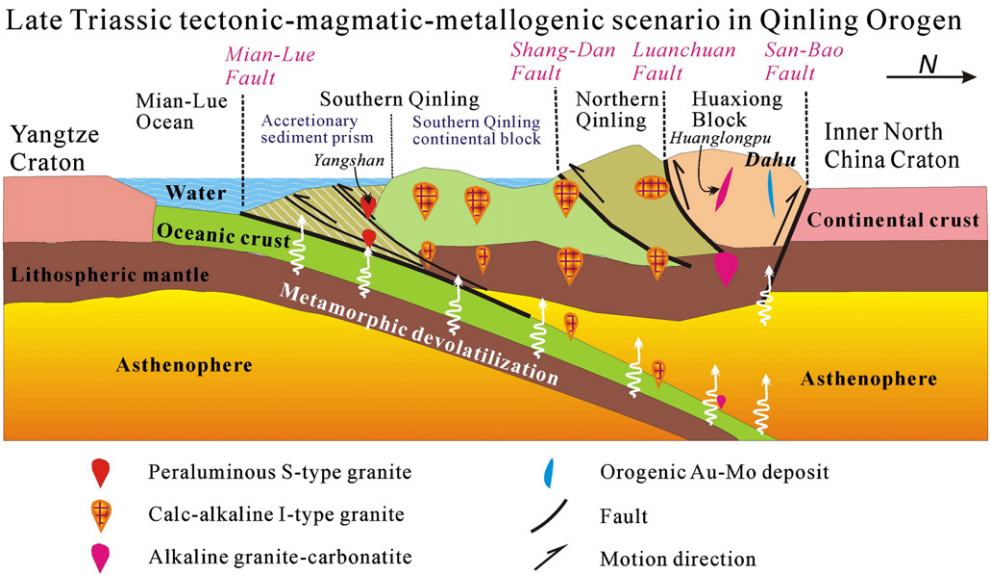

Fig. 5. Triassic tectonic–magmatic–metallogenic scenario in the Qinling Orogen.

model involving the northward oceanic plate subduction along the Mian-Lue suture. In Triassic, the Mian-Lue Ocean was not completely closed, and the oceanic plate subduction was still active.

Acknowledgments

This study is financially granted by NSFC (Nos. 41003019 and 40730421), and the National 973-program (No. 2006CB403508). The authors are also grateful to the Henan Institute of Geology Survey and the Henan Institute of Nonferrous Metal Exploration for assistance during the field trip. Reviews by Professor S.Y. Jiang and Dr. H.Y. Chen have greatly improved the quality of our paper.

References

Chen, Y.J., 2010. Indosinian tectonic setting, magmatism and metallogenesis in Qinling Orogen, central China. Geol. China 37, 854–865 (in Chinese with English abstract).
Chen, Y.J., Fu, S.G., 1992. Gold Mineralization in West Henan. Seismological Press, Beijing. 234 pp. (in Chinese with English abstract).
Chen, Y.J., Zhao, Y.C., 1997. Geochemical characteristics and evolution of REE in the Early Precambrian sediments: evidences from the southern margin of the North China craton. Episodes 20, 109–116.
Chen, Y.J., Guo, G.J., Li, X., 1998. Metallogenic geodynamic background of gold deposits in Granite-greenstone terrains of North China craton. Sci. China D 41, 113–120.
Chen, Y.J., Li, C., Zhang, J., Li, Z., Wang, H.H., 2000. Sr and O isotopic characteristics of porphyries in the Qinling molybdenum deposit belt and their implication to genetic mechanism and type. Sci. China D 43, 82–94 (Suppl.).
Chen, Y.J., Pirajno, F., Sui, Y.H., 2005. Geology and D–O–C isotope systematics of the Tieluping silver deposit, Henan, China: implications for ore genesis. Acta Geol. Sin. 79, 106–119.
Chen, Y.J., Pirajno, F., Qi, J.P., 2008. The Shanggong gold deposit, eastern Qinling Orogen, China: Isotope geochemistry and implications for ore genesis. J. Asian Earth Sci. 33, 252–266.
Chen, Y.J., Pirajno, F., Li, N., Guo, D.S., Lai, Y., 2009. Isotope systematics and fluid inclusion studies of the Qiyugou breccia pipe-hosted gold deposit, Qinling Orogen, Henan province, China: implications for ore genesis. Ore Geol. Rev. 35, 245–261.
Deng, X.H., Yao, J.M., Jing, L., Li, S.Y., 2009. Molybdenite Re–Os isotope age of the Zhaiwa Mo deposit and implications for Xiongerian mineralization in eastern Qinling Orogen. Acta Petrol. Sin. 25, 2739–2746 (in Chinese with English abstract).
Depaolo, D.J., Wasserburg, G.J., 1979. Petrogenetic mixing models and Nd–Sr isotopic patterns. Geochim. Cosmochim. Acta 43, 615–627.
Gong, H.J., Zhu, L.M., Sun, B.Y., Li, B., Guo, B., 2009. Zircon U–Pb ages and Hf isotope characteristics and their geological significance of the Shahewan, Caoping and Zhashui granitic plutons in the South Qinling orogen. Acta Petrol. Sin. 25, 248–264 (in Chinese with English abstract).
Hagemann, S.G., Cassidy, K.F., 2000. Archean orogenic lode gold deposits. Rev. Econ. Geol. 13, 9–68.
Hoefs, J., 1997. Stable Isotope Geochemistry, Forth edition. Springer-Verlag, Berlin. (201 pp.).
Hu, S.X., 1988. Geology and Metallogeny of the Collision Belt Between the South China and North China Plates. Nanjing University Press, Nanjing. 558 pp. (in Chinese).
Jacobsen, S.B., Wasserburg, G.J., 1980. Nd isotopic evolution of chondrites. Earth Planet. Sci. Lett. 50, 139–155.
Jiang, S.Y., Dai, B.Z., Jiang, Y.H., Zhao, H.X., Hou, M.L., 2009. Jiaodong and Xiaoqinling: two orogenic gold provinces formed in different tectonic settings. Acta Petrol. Sin. 25, 2727–2738 (in Chinese with English abstract).
Jiang, Y.H., Jin, G.D., Liao, S.Y., Zhou, Q., Zhao, P., 2010. Geochemical and Sr–Nd–Hf isotopic constraints on the origin of Late Triassic granitoids from the Qinling orogen, central China: Implications for a continental arc to continent–continent collision. Lithos 117, 183–197.
Kerrich, R., Goldfarb, R.J., Groves, D., Garwin, S., Jia, Y.F., 2000. The characteristics, origins, and geodynamic settings of supergiant gold metallogenic provinces. Sci. China D Earth Sci. 43, 1–68 (Suppl.).
Li, N., Chen, Y.J., Zhang, H., Zhao, T.P., Deng, X.H., Wang, Y., Ni, Z.Y., 2007. Molybdenum deposits in East Qinling. Earth Sci. Front. 14, 186–198 (in Chinese with English abstract).
Li, N., Sun, Y.L., Li, J., Xue, L.W., Li, W.B., 2008. The molybdenite Re–Os isotope age of the Dahu Au Mo deposit, Xiaoqinling and the Indosinian mineralization. Acta Petrol. Sin. 24, 810–816 (in Chinese with English abstract).
Li, N., Chen, Y.J., Fletcher, I.R., Zeng, Q.T., 2011a. Triassic mineralization with Cretaceous overprint in the Dahu Au–Mo deposit, Xiaoqinling gold province: constraints from SHRIMP monazite U–Th–Pb geochronology. Gondwana Res. 20, 543–552.
Li, N., Chen, Y.J., Santosh, M., Yao, J.M., Sun, Y.L., Li, J., 2011b. The 1.85 Ga Mo mineralization in the Xiong'er Terrane, China: implications for metallogeny associated with assembly of the Columbia supercontinent. Precambrian Res. 186, 220–232.
Liu, H.J., Chen, Y.J., Mao, S.D., Zhao, C.H., Yang, R.S., 2008. Element and Sr–Nb–Pb isotope geochemistry of granite-porphyry dykes in the Yangshan gold belt, western Qinling orogen. Acta Petrol. Sin. 24, 1101–1111 (in Chinese with English abstract).
Mao, J.W., Goldfarb, R.J., Zhang, Z.W., Xu, W.Y., Qiu, Y.M., Deng, J., 2002. Gold deposits in the Xiaoqinling-Xiong'ershan region, Central China. Miner. Deposita 37, 306–325.
Mao, J.W., Xie, G.Q., Bierlein, F., Qü, W.J., Du, A.D., Ye, H.S., Pirajno, F., Li, H.M., Guo, B.J., Li, Y.F., Yang, Z.Q., 2008. Tectonic implications from Re–Os dating of Mesozoic molybdenum deposits in the East Qinling-Dabie orogenic belt. Geochim. Cosmochim. Acta 72, 4607–4626.
Ni, Z.Y., Li, N., Guan, S.J., Zhang, H., Xue, L.W., 2008. Characteristics of fluid inclusions and ore genesis of the Dahu Au–Mo deposit in the Xiaoqinling gold field, Henan province. Acta Petrol. Sin. 24, 2058–2068 (in Chinese with English abstract).
Pirajno, F., 2009. Hydrothermal Processes and Mineral Systems. Springer, Berlin. (1250 pp.).
Tanaka, T., Togashi, S., Kamioka, H., Amakawa, H., Kagami, H., Hamamoto, T., Yuhara, M., Orihashi, Y., Yoneda, S., Shimizu, H., Kunimaru, T., Takahashi, K., Yanagi, T., Nakano, T., Fujimaki, H., Shinjo, R., Asahara, Y., Tanimizu, M., Dragusanu, C., 2000. JNdi-1: a neodymium isotopic reference in consistency with LaJolla neodymium. Chem. Geol. 168, 279–281.
Taylor, H.P., 1974. The application of oxygen and hydrogen isotope studies to problems of hydrothermal alteration and ore deposition. Econ. Geol. 69, 843–883.
Xu, C., Kynicky, J., Chakhmouradian, A.R., Qi, L., Song, W.L., 2010. A unique Mo deposit associated with carbonatites in the Qinling orogenic belt, central China. Lithos 118, 50–60.
Zartman, R.E., Doe, B.R., 1981. Plumbotectonics — the model. Tectonophysics 75, 135–162.
Zhang, J.J., Zheng, Y.D., Liu, S.W., 1998. Structure, Genetic Mechanism and Evolution of the Xiaoqinling Metamorphic Core Complex. China Ocean Press, Beijing. (in Chinese with English abstract).
Zhang, G.W., Zhang, B.R., Yuan, J.C., Xiao, Q.H., 2001. The Qinling Orogenic Belt and Continental Dynamics. Science Press, Beijing. 855 pp. (in Chinese).

Zhang, B.R., Gao, S., Zhang, H.F., Han, Y.W., 2002. Geochemistry of the Qinling Orogen. Science Press, Beijing. 187 pp. (in Chinese).
Zhang, L., Yang, R.S., Mao, S.D., Lu, Y.H., Qin, Y., Liu, H.J., 2009a. Sr and Pb isotope geochemistry and ore-forming material source of the Yangshan gold deposit. Acta Petrol. Sin. 25, 2811–2822 (in Chinese with English abstract).
Zhang, Y.H., Li, Z.Y., Zhang, X.M., Qian, M.P., Yang, Z.Q., He, Y., Zhang, S.M., Zhang, L.Z., Wang, J.M., 2009b. Overthrust development and its relationship to gold mineralization in the northern belt of the Xiaoqinling gold (molybdenum) province, Central China. J. Jilin Univ. (Earth Sci. Ed.) 39, 244–254 (in Chinese with English abstract).
Zhao, G.C., He, Y.H., Sun, M., 2009. The Xiong'er volcanic belt at the southern margin of the North China Craton: Petrographic and geochemical evidence for its outboard position in the Paleo-Mesoproterozoic Columbia Supercontinent. Gondwana Res. 17, 145–152.
Zhao, H.X., Hartwig, E.F., Jiang, S.Y., Dai, B.-Z., 2011. LA-ICP-MS trace element analysis of pyrite from the Xiaoqinling gold district, China: implications for ore genesis. Ore Geol. Rev. 43, 142–153.
Zhao, H.X., Jiang, S.Y., Hartwig, E.F., Dai, B.Z., Ma, L., 2012. Geochemistry, geochronology and Sr–Nd–Hf isotopes of two Mesozoic granitoids in the Xiaoqinling gold district: implication for large-scale lithospheric thinning in the North China Craton. Chem. Geol. doi:10.1016/j.chemgeo.2011.11.030
Zheng, Y.F., 1999. Stable isotope geochemistry. In: Zheng, Y.F. (Ed.), Chemical Geodynamics. Science Press, Beijing, pp. 62–118.
Zhu, L.M., Zhang, G.W., Chen, Y.J., Ding, Z.J., Guo, B., Wang, F., Lee, B., 2011. Zircon U–Pb ages and geochemistry of the Wenquan Mo-bearing granitioids in West Qinling, China: constraints on the geodynamic setting for the newly discovered Wenquan Mo deposit. Ore Geol. Rev. 39, 49–62.